

## Complex Hydrides with $(\text{BH}_4)^-$ and $(\text{NH}_2)^-$ Anions as New Lithium Fast-Ion Conductors

Motoaki Matsuo,<sup>†</sup> Arndt Remhof,<sup>‡</sup> Pascal Martelli,<sup>‡</sup> Riccarda Caputo,<sup>‡</sup> Matthias Ernst,<sup>§</sup> Yohei Miura,<sup>†</sup> Toyoto Sato,<sup>†</sup> Hiroyuki Oguchi,<sup>†,||</sup> Hideki Maekawa,<sup>||</sup> Hitoshi Takamura,<sup>||</sup> Andreas Borgschulte,<sup>‡</sup> Andreas Züttel,<sup>‡</sup> and Shin-ichi Orimo<sup>\*,†</sup>

*Institute for Materials Research, Tohoku University, Katahira 2-1-1, Sendai, 980-8577, Japan, EMPA, Department Environment, Energy and Mobility, Abt. 138 "Hydrogen & Energy", Überlandstrasse 129, 8600 Dübendorf, Switzerland, ETH Zürich, Physical Chemistry, Wolfgang-Pauli-Strasse 10, 8093 Zürich, Switzerland, and Graduate School of Engineering, Tohoku University, Aramaki Aza Aoba 6-6-02, Sendai, 980-8579, Japan*

Received August 27, 2009; E-mail: orimo@imr.tohoku.ac.jp

Complex hydrides with the  $(\text{BH}_4)^-$  anion are conventionally expressed as  $M(\text{BH}_4)_n$  ( $n$ : valence of metal  $M$ ), which shows ionic bonding between the  $M^{n+}$  cation and the  $(\text{BH}_4)^-$  anion. These hydrides have been attracting great interest as potential candidates for advanced hydrogen storage materials because of their high hydrogen densities.<sup>1,2</sup> Moreover, some of the authors have reported that one of the complex hydrides,  $\text{Li}(\text{BH}_4)$ , exhibits another novel chemical property, that is, lithium fast-ion conduction (more than  $1 \times 10^{-3}$  S/cm over 390 K),<sup>3</sup> which was observed during attempts to clarify the microwave absorbing mechanism.<sup>4,5</sup> Although a wide variety of inorganic lithium fast-ion conductors such as oxides<sup>6–8</sup> and sulfides<sup>9–12</sup> have been reported, no lithium fast-ion conductor of hydride except  $\text{Li}(\text{BH}_4)$  has been found since the report of  $\text{Li}_2(\text{NH})$  in 1979.<sup>13</sup> The research and development of lithium (fast-)ion conductors is significantly important because they may potentially be applied to solid electrolytes to improve safety and energy-density related issues of conventional lithium-ion batteries.

The ion conductivity of  $\text{Li}(\text{BH}_4)$  increases by 3 orders of magnitude at  $\sim 390$  K due to its structural transition from the low temperature (LT) phase to the high temperature (HT) phase.<sup>3</sup> Also it has been recently demonstrated that the HT phase of  $\text{Li}(\text{BH}_4)$  can be stabilized by addition of lithium halides, resulting in the enhanced conductivity at room temperature (RT).<sup>14–16</sup>

Here we report another conceptual study and remarkable results of  $\text{Li}_2(\text{BH}_4)(\text{NH}_2)$  and  $\text{Li}_4(\text{BH}_4)(\text{NH}_2)_3$  combined with the  $(\text{BH}_4)^-$  and  $(\text{NH}_2)^-$  anions showing ion conductivities 4 orders of magnitude higher than that for  $\text{Li}(\text{BH}_4)$  at RT, due to being provided with new occupation sites for  $\text{Li}^+$  ions. This study not only demonstrates an important direction in which to search for higher ion conductivity in complex hydrides but also greatly increases the material variations of solid electrolytes.

Experimental details are given in the Supporting Information. Briefly, the complex hydrides were synthesized by mechanical milling of two host hydrides, 1 M of  $\text{Li}(\text{BH}_4)$  and  $x$  M of  $\text{Li}(\text{NH}_2)$  with  $x = 1$  and 3. Following heat treatment for sufficient crystalline growth (crystallite sizes: more than 100–200 nm), the resulting powders were subjected to electrical conductivity measurements by an ac impedance method. Temperature ranges for the conductivity measurement were from RT to above and

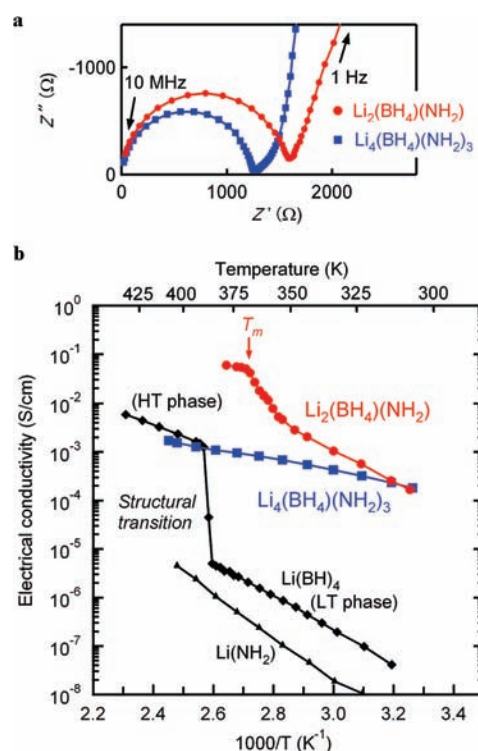


**Figure 1.** Electrical properties of  $\text{Li}_2(\text{BH}_4)(\text{NH}_2)$  and  $\text{Li}_4(\text{BH}_4)(\text{NH}_2)_3$  measured in heating run. (a) Typical impedance plots obtained using a molybdenum–metal electrode at RT. (b) Arrhenius plots of the electrical conductivities. The melting temperature of  $\text{Li}_2(\text{BH}_4)(\text{NH}_2)$ , 365 K, is indicated as  $T_m$ . For reference, the data of  $\text{Li}(\text{BH}_4)$  and  $\text{Li}(\text{NH}_2)$  as host hydrides are also shown.

below melting temperatures for  $\text{Li}_2(\text{BH}_4)(\text{NH}_2)$  and  $\text{Li}_4(\text{BH}_4)(\text{NH}_2)_3$ , respectively.

The electrical conductivities of  $\text{Li}_2(\text{BH}_4)(\text{NH}_2)$  and  $\text{Li}_4(\text{BH}_4)(\text{NH}_2)_3$  were determined from their impedance plots. Figure 1a shows typical plots obtained using a molybdenum–metal electrode. The plot of  $\text{Li}_2(\text{BH}_4)(\text{NH}_2)$  showed a spike in the lower frequency range caused by the electrode contribution as well as a semicircle in the higher frequency range. It has been confirmed that the plot obtained using a lithium–metal electrode exhibited only the semicircle, which is interpreted as being a parallel combination of resistance and capacitance. The capacitance was found to be 160 pF, which is consistent with the bulk contribution

<sup>†</sup> Institute for Materials Research, Tohoku University.

<sup>‡</sup> EMPA.

<sup>§</sup> ETH Zürich.

<sup>||</sup> Graduate School of Engineering, Tohoku University.

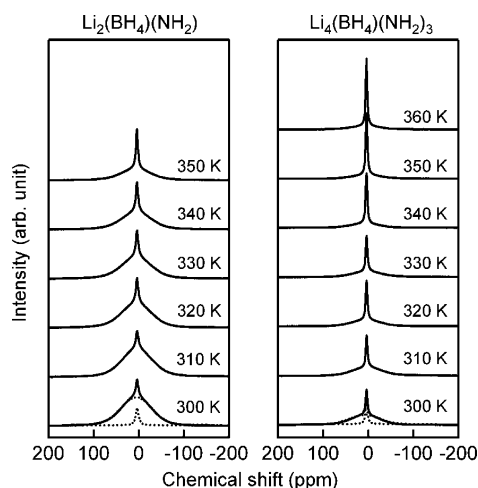


**Figure 2.**  $^7\text{Li}$  NMR spectra of  $\text{Li}_2(\text{BH}_4)(\text{NH}_2)$  and  $\text{Li}_4(\text{BH}_4)(\text{NH}_2)_3$  at some selected temperatures (below their melting temperatures), measured in heating run. Representative Lorentzian component and Gaussian component are shown by dotted lines in spectra at 300 K.

in  $\text{Li}(\text{BH}_4)$  (100–300 pF).<sup>3</sup> The hydride was heat-treated for the sufficient crystal growth as mentioned above, so the grain boundary contribution was not observed, which is the same tendency as in the case of  $\text{Li}(\text{BH}_4)$ .<sup>15</sup> A similar impedance plot was also observed for  $\text{Li}_4(\text{BH}_4)(\text{NH}_2)_3$ . Both of the plots shown in Figure 1a represent the characteristics of ion conductors composed of the bulk and electrode contributions.

As shown in Figure 1b,  $\text{Li}_2(\text{BH}_4)(\text{NH}_2)$  exhibited a fast-ion conductivity of  $2 \times 10^{-4}$  S/cm at RT, which is 4 and 5 orders of magnitude higher than those of the host hydrides  $\text{Li}(\text{BH}_4)$  and  $\text{Li}(\text{NH}_2)$ , respectively, and the conductivity monotonically increased upon heating. The activation energy for conduction significantly decreased at  $\sim 368$  K from 0.56 eV (303–348 K) to 0.24 eV (above 368 K). From the differential scanning calorimetry (DSC) measurement, the melting temperature of  $\text{Li}_2(\text{BH}_4)(\text{NH}_2)$  was estimated to be 365 K (see Figure S1 in the Supporting Information). Therefore, the significant change in the activation energy at 368 K shown in Figure 1b is attributed to the melting of  $\text{Li}_2(\text{BH}_4)(\text{NH}_2)$ .<sup>17</sup> The total ion conductivity<sup>18</sup> reached up to  $6 \times 10^{-2}$  S/cm after melting at the highest temperature measured in this study, 378 K.  $\text{Li}_4(\text{BH}_4)(\text{NH}_2)_3$  also exhibited high ion conductivities of  $2 \times 10^{-4}$  S/cm even at RT, and the value reached  $1 \times 10^{-3}$  S/cm at  $\sim 370$  K. The activation energy for conduction was evaluated to be 0.26 eV. It is noteworthy that this value is less than half those in  $\text{Li}_2(\text{BH}_4)(\text{NH}_2)$  before melting and  $\text{Li}(\text{BH}_4)$  (LT phase: 0.69 eV, HT phase: 0.53 eV).<sup>3</sup> X-ray diffraction (XRD) analysis revealed that no significant changes in the interface between the hydrides and the lithium–metal electrode took place before and after the ac impedance measurements (see Figure S2 in the Supporting Information).

The dynamics of  $\text{Li}^+$  ions can be studied by  $^7\text{Li}$  nuclear magnetic resonance (NMR) spectroscopy. Figure 2 shows the spectra at some selected temperatures below their melting temperatures. The narrowing of the line widths, so-called motional narrowing, was observed even at RT for both  $\text{Li}_2(\text{BH}_4)(\text{NH}_2)$  and  $\text{Li}_4(\text{BH}_4)(\text{NH}_2)_3$ , indicating the high mobility of  $\text{Li}^+$  ions in the complex hydrides at RT. The overlapping of a broad Gaussian component and a sharp Lorentzian component suggests the existence of the  $\text{Li}^+$  ions with low mobility as well as those with high mobility,<sup>19</sup> which we attribute to the local atomistic structures of the hydrides.

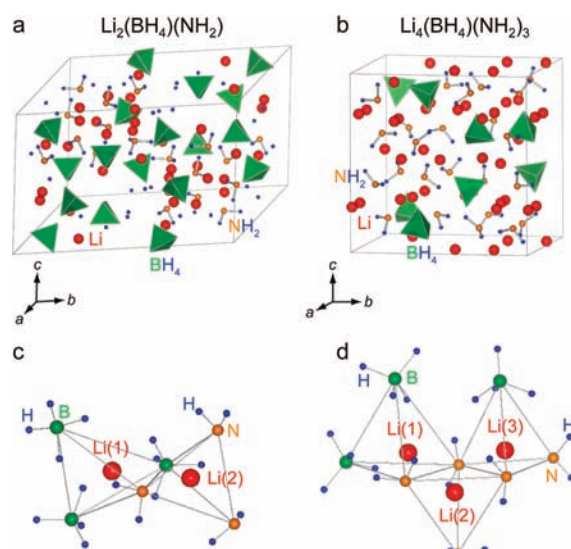


**Figure 3.** Crystal structures of (a)  $\text{Li}_2(\text{BH}_4)(\text{NH}_2)$  and (b)  $\text{Li}_4(\text{BH}_4)(\text{NH}_2)_3$  mainly on the basis of Wu et al.<sup>23</sup> (c), (d) Plural occupation sites for  $\text{Li}^+$  ions in the hydrides. Red, green, orange and blue solid circles show Li, B, N and H, respectively. The green tetrahedrons show the  $(\text{BH}_4)^-$  anion.  $\text{Li}_2(\text{BH}_4)(\text{NH}_2)$  has two Li-18f sites; Li(1) is tetrahedrally coordinated by  $3(\text{BH}_4)^- + 1(\text{NH}_2)^-$  and Li(2) by  $1(\text{BH}_4)^- + 3(\text{NH}_2)^-$ . On the other hand,  $\text{Li}_4(\text{BH}_4)(\text{NH}_2)_3$  has two Li-12b and one Li-8a sites; Li(1) is tetrahedrally coordinated by  $2(\text{BH}_4)^- + 2(\text{NH}_2)^-$ , Li(2) by  $4(\text{NH}_2)^-$  and Li(3) by  $1(\text{BH}_4)^- + 3(\text{NH}_2)^-$ .

Actually, the crystal structures of  $\text{Li}_2(\text{BH}_4)(\text{NH}_2)$  and  $\text{Li}_4(\text{BH}_4)(\text{NH}_2)_3$  have been recently investigated from the viewpoint of developing hydrogen storage materials.<sup>20–23</sup> As shown in Figure 3, both  $\text{Li}_2(\text{BH}_4)(\text{NH}_2)$  and  $\text{Li}_4(\text{BH}_4)(\text{NH}_2)_3$  have plural occupation sites for  $\text{Li}^+$  ions with differing tetrahedral coordination consisting of  $(\text{BH}_4)^-$  and  $(\text{NH}_2)^-$  anions.<sup>23</sup>  $\text{Li}_2(\text{BH}_4)(\text{NH}_2)$  has 18 Li(1)s and 18 Li(2)s per unit cell, while  $\text{Li}_4(\text{BH}_4)(\text{NH}_2)_3$  has 12 Li(1)s, 12 Li(2)s, and 8 Li(3)s. Here, calculating the size of each occupation site is important because qualitatively it can be a useful factor in estimating the size of the bottleneck for  $\text{Li}^+$  ion diffusion. We calculated the size of each site, which was defined as the maximum radius of a sphere surrounded by the neighboring H atoms of  $(\text{BH}_4)^-$  and  $(\text{NH}_2)^-$  anions,<sup>24</sup> as follows: Li(1), 0.16 nm and Li(2), 0.09 nm in  $\text{Li}_2(\text{BH}_4)(\text{NH}_2)$  and Li(1), 0.17 nm; Li(2), 0.11 nm; and Li(3), 0.11 nm in  $\text{Li}_4(\text{BH}_4)(\text{NH}_2)_3$ . It is interesting to note that in  $\text{Li}_2(\text{BH}_4)(\text{NH}_2)$  50%  $\text{Li}^+$  ions occupy the rather small Li(2) [ $\sim 56\%$  in radius and 18% in volume of the Li(1)]. The higher ratio of the peak area of the Gaussian component against the Lorentzian component, and also the larger activation energy for conduction, for  $\text{Li}_2(\text{BH}_4)(\text{NH}_2)$  than for  $\text{Li}_4(\text{BH}_4)(\text{NH}_2)_3$  can be explained by the  $\text{Li}^+$  ions with lower mobility in the Li(2). Detailed measurements using high-resolution NMR are now underway.

It should be strongly emphasized that, although the crystal structures of  $\text{Li}_2(\text{BH}_4)(\text{NH}_2)$  (trigonal,  $R\bar{3}$ ,  $a = 1.4492(1)$ ,  $c = 0.9236(1)$  nm) and  $\text{Li}_4(\text{BH}_4)(\text{NH}_2)_3$  (cubic,  $I2_3$ ,  $a = 1.0669(1)$  nm) are rather different from the LT phase (orthorhombic,  $Pnma$ ,  $a = 0.717858(4)$ ,  $b = 0.443686(2)$ ,  $c = 0.680321(4)$  nm), the HT phase (hexagonal,  $P6_3mc$ ,  $a = 0.427631(5)$ ,  $c = 0.694844(8)$  nm) of  $\text{Li}(\text{BH}_4)$ ,<sup>25</sup> and  $\text{Li}(\text{NH}_2)$  (tetragonal,  $\bar{4}$ ,  $a = 0.503442(24)$ ,  $c = 1.025558(52)$  nm),<sup>26</sup> the combinations of anions containing hydrogen [the  $(\text{BH}_4)^-$  and  $(\text{NH}_2)^-$  anions in this study] could provide new occupation sites for  $\text{Li}^+$  ions which are appropriate for their high mobility. There are various other anions containing

hydrogen such as  $(\text{AlH}_4)^-$ ,  $(\text{NH})^{2-}$ ,  $(\text{AlH}_6)^{3-}$ , and  $(\text{NiH}_4)^{4-}$ ; further combinations of these anions should greatly enlarge the material variations of lithium fast-ion conductors for possible solid electrolytes. Furthermore, there is a strong probability of close interactions between the high mobility of  $\text{Li}^+$  ions and the B–H dynamics in the  $(\text{BH}_4)^-$  anions and/or N–H dynamics in the  $(\text{NH}_2)^-$  anions in the hydrides; we have experimentally confirmed that the activation energy for hydrogen reorientational motion in the  $(\text{BH}_4)^-$  anion<sup>27–30</sup> obtained by  $^1\text{H}$  NMR (0.69 eV) was in good agreement with that for the lithium ion conduction (0.67 eV) in the  $\text{Li}(\text{BH}_4)$ -based system.<sup>14</sup> Detailed studies using high-resolution NMR and neutron diffraction/scattering are now being conducted.

In summary, we have reported the discovery of novel lithium fast-ion conductors of complex hydrides consisting of combinations of the  $(\text{BH}_4)^-$  and  $(\text{NH}_2)^-$  anions, that is,  $\text{Li}_2(\text{BH}_4)(\text{NH}_2)$  and  $\text{Li}_4(\text{BH}_4)(\text{NH}_2)_3$ .  $\text{Li}_2(\text{BH}_4)(\text{NH}_2)$  exhibited a lithium fast-ion conductivity of  $2 \times 10^{-4}$  S/cm even at RT, which is 4 orders of magnitude higher than that of  $\text{Li}(\text{BH}_4)$ . Upon heating, the activation energy for conduction decreased significantly from 0.56 eV (303–348 K) to 0.24 eV (above 368 K) due to melting, and the total ion conductivity reached up to  $6 \times 10^{-2}$  S/cm at 378 K.  $\text{Li}_4(\text{BH}_4)(\text{NH}_2)_3$  also exhibited a high ion conductivity of  $2 \times 10^{-4}$  S/cm at RT, and the value reached  $1 \times 10^{-3}$  S/cm at  $\sim 370$  K. The activation energy for conduction in  $\text{Li}_4(\text{BH}_4)(\text{NH}_2)_3$  was evaluated to be 0.26 eV, less than half those in  $\text{Li}_2(\text{BH}_4)(\text{NH}_2)$  (below the melting temperature) and  $\text{Li}(\text{BH}_4)$  (LT phase: 0.69 eV, HT phase: 0.53 eV). We note that combinations of complex anions containing hydrogen [the  $(\text{BH}_4)^-$  and  $(\text{NH}_2)^-$  anions in this study] could provide new occupation sites for  $\text{Li}^+$  ions which are appropriate for their high mobility and, thus, could greatly increase the material variations of lithium fast-ion conductors for possible solid electrolytes.

**Acknowledgment.** We would like to thank Professor Beat H. Meier, ETH Zurich, for measurement time on the solid-state NMR spectrometer and the computer facilities at EMPA. Financial support by Global COE Program “Materials Integration, Tohoku University,” MEXT, Japan (M.M., T.S., H.T., and S.O.), Swiss National Science Foundation (Project No. 200021-119972) (A.R., P.M., and A.Z.), KAKENHI Creative Scientific Research Program “Study of nano-energy system creation” (H.O. and S.O.), KAKENHI Grant-in-Aid for Scientific Research No. 21246100 (M.M., H.M., H.T., and S.O.), NEDO “Advanced Fundamental Research Project on Hydrogen Storage Materials” (H.M. and H.T.), and Integrated Project of ICC-IMR, Tohoku University (A.Z. and S.O.) is greatly appreciated.

**Supporting Information Available:** Experimental procedures, DSC, XRD, and Raman data. This material is available free of charge via the Internet at <http://pubs.acs.org>.

## References

- (1) Orimo, S.; Nakamori, Y.; Eliseo, J. R.; Züttel, A.; Jensen, C. M. *Chem. Rev.* **2007**, *107*, 4111–4132.
- (2) Züttel, A.; Borgschulte, A.; Orimo, S. *Scr. Mater.* **2007**, *56*, 823–828.
- (3) Matsuo, M.; Nakamori, Y.; Orimo, S.; Maekawa, H.; Takamura, H. *Appl. Phys. Lett.* **2007**, *91*, 224103.
- (4) Nakamori, Y.; Orimo, S.; Tsutaoka, T. *Appl. Phys. Lett.* **2006**, *88*, 112104.
- (5) Matsuo, M.; Nakamori, Y.; Yamada, K.; Orimo, S. *Appl. Phys. Lett.* **2007**, *90*, 232907.
- (6) Aono, H.; Sugimoto, E.; Sadaoka, Y.; Imanaka, N.; Adachi, G. J. *Electrochem. Soc.* **1993**, *140*, 1827–1833.
- (7) Inaguma, Y.; Liqun, C.; Itoh, M.; Nakamura, T.; Uchida, T.; Ikuta, H.; Wakihara, M. *Solid State Commun.* **1993**, *86*, 689–693.
- (8) Martínez-Juárez, A.; Rojo, J. M.; Iglesias, J. E.; Sanz, J. *Chem. Mater.* **1995**, *7*, 1857–1862.
- (9) Tachez, M.; Malugani, J. P.; Mercier, R.; Robert, G. *Solid State Ionics* **1984**, *14*, 181–185.
- (10) Takada, K.; Aotani, N.; Iwamoto, K.; Kondo, S. *Solid State Ionics* **1996**, *86–88*, 877–882.
- (11) Kanno, R.; Murayama, M. *J. Electrochem. Soc.* **2001**, *148*, A742–A746.
- (12) Mizuno, F.; Hayashi, A.; Tadanaga, K.; Tatsumisago, M. *Adv. Mater.* **2005**, *17*, 918–921.
- (13) Boukamp, B. A.; Huggins, R. A. *Phys. Lett. A* **1979**, *72*, 464–466.
- (14) Maekawa, H.; Matsuo, M.; Takamura, H.; Ando, M.; Noda, Y.; Karahashi, T.; Orimo, S. *J. Am. Chem. Soc.* **2009**, *131*, 894–895.
- (15) Matsuo, M.; Takamura, H.; Maekawa, H.; Li, H. -W.; Orimo, S. *Appl. Phys. Lett.* **2009**, *94*, 084103.
- (16) Oguchi, H.; Matsuo, M.; Hummelshøj, J. S.; Vegge, T.; Nørskov, J. K.; Sato, T.; Miura, Y.; Takamura, H.; Maekawa, H.; Orimo, S. *Appl. Phys. Lett.* **2009**, *94*, 141912.
- (17) As shown in Figure S1 in the Supporting Information, a small endothermic peak at 360–365 K was observed before melting at 365 K during heating in the DSC curve of  $\text{Li}_2(\text{BH}_4)(\text{NH}_2)$ , which might be due to the formation of a new decomposition phase. The increase of the activation energy between 350 and 368 K may be related to the phase.
- (18) The conductivity is associated with only the lithium ion conduction in the solid state  $\text{Li}_2(\text{BH}_4)(\text{NH}_2)$  before melting, while the contribution of the anions is presumably included after melting.
- (19) Xia, Y.; Machida, N.; Wu, X.; Lakeman, C.; Willen, L.; Lange, F.; Levi, C.; Eckert, H. *J. Phys. Chem. B* **1997**, *101*, 9180–9187.
- (20) Aoki, M.; Miwa, K.; Noritake, T.; Kitahara, G.; Nakamori, Y.; Orimo, S.; Towata, S. *Appl. Phys. A* **2005**, *80*, 1409–1412.
- (21) Pinkerton, F. E.; Meisner, G. P.; Meyer, M. S.; Balogh, M. P.; Kundrat, M. D. *J. Phys. Chem. B* **2005**, *109*, 6–8.
- (22) Chater, P. A.; David, W. I. F.; Johnson, S. R.; Edwards, P. P.; Anderson, P. A. *Chem. Commun.* **2006**, *23*, 2439–2441.
- (23) Wu, H.; Zhou, W.; Udovic, T. J.; Rush, J. J.; Yildirim, T. *Chem. Mater.* **2008**, *20*, 1245–1247.
- (24) Calculation was conducted with the program MedeA (Materials Design, Inc., version 2.4.7, <http://www.materialsdesign.com/medea>).
- (25) Soulié, J.-P.; Renaudin, G.; Cerny, R.; Yvon, K. *J. Alloys Compd.* **2002**, *346*, 200–205.
- (26) Yang, J. B.; Zhou, X. D.; Cai, Q.; James, W. J.; Yelon, W. B. *Appl. Phys. Lett.* **2006**, *88*, 041914.
- (27) Hagemann, H.; Gomes, S.; Renaudin, G.; Yvon, K. *J. Alloys Compd.* **2004**, *363*, 126–129.
- (28) Hartman, M. R.; Rush, J. J.; Udovic, T. J.; Bowman, R. C., Jr.; Hwang, S.-J. *J. Solid State Chem.* **2007**, *180*, 1298–1305.
- (29) Filinchuk, Y.; Chernyshov, D.; Cerny, R. *J. Phys. Chem. C* **2008**, *112*, 10579–10584.
- (30) Buchter, F.; Łodziana, Z.; Mauron, Ph.; Remhof, A.; Friedrichs, O.; Borgschulte, A.; Züttel, A.; Sheptyakov, D.; Strässle, Th.; Ramirez-Cuesta, A. *J. Phys. Rev. B* **2008**, *78*, 094302.

JA907249P